Journal of Applied Sciences

ISSN 1812-5654

science alert

ANSInet
an open access publisher
http://ansinet.com

Journal of Applied Sciences 9 (9): 1628-1646, 2009
ISSN 1812-5654

Geochemistry, Mineralization and Alteration Zones of Darrehzar Porphyry Copper Deposit, Kerman, Iran

[1]R. Derakhshani and [2]M. Abdolzadeh
[1]Department of Geology, Shahid Bahonar University, Kerman, Iran
[2]Department of Environment of Kerman Province, Havaniruz Street, Kerman, Iran

Abstract: The goal of this study is focused on alteration, mineralization and geochemistry of Darrehzar porphyry copper deposit which is situated in the Central Iranian Tectono-Volcanic Belt. This deposit is associated with an Oligocene granodiorite stock which intruded Eocene Volcano-Sedimentary and Cretaceous carbonate rocks. Four distinct types of hypogene alterations are recognized at Darrehzar: potassic, phyllic, argillic and propylitic. Copper mineralization was accompanied mainly by phyllic and to a lesser extent potassic, alteration. In the potassic alteration zone, enrichment of K and depletion of Na, Ca, Mn and Fe took place. These changes attended replacement of plagioclase and amphibole by K-feldspar and biotite, respectively. Potassic alteration was associated with a major addition of Cu, as evident from the occurrence of disseminated chalcopyrite and bornite in this zone. Phyllic alteration was accompanied by depletion of Na, K, Fe and Ba and enrichment of Si and Cu. Losses of Na, K and Fe reflect sericitization of alkali feldspar and destruction of ferromagnesian minerals. The addition of Si is consistent with widespread silicification, which is a major feature of phyllic alteration, as well as the addition of Cu mobilized from the potassic zone. Pertographic studies of this porphyry copper deposit indicate that granodiorite association is mainly composed of plagioclase, quartz, orthoclase, biotite, sericite. The main mineralization-related alteration episodes (potassic, phyllic, argillic, propylitic) have been studied in terms of mass transfer and element mobility during the hydrothermal evolution of the Darrehzar copper deposit.

Key words: Mass change, hypogene, potassic, phyllic, argillic, propylitic

INTRODUCTION

Darrehzar deposit (Fig. 1) is located in Central Iranian Volcanic Belt (Ranjbar *et al*., 2004) as well as other porphyry copper deposits of Iran, like Sarcheshmeh and Sungun (Hezarkhani, 1998). This zone which also is known as Urumieh-Dokhtar magmatic assemblage (Shahabpour, 1991) is aligned parallel to the Zagros Thrust Zone and also to the prevalent fold axes in the Zagros Mountain Range (Regards *et al*., 2004, 2005; Berberian, 1995; Amidi *et al*., 1984).

The magmatic processes and associated mineralization in this belt are thought to be related to subduction along the Zagros Thrust Zone (Forster, 1978; Shahabpour and Kramers, 1987; Shahabpour and Doorandish, 2008; Derakhshani and Farhoudi, 2005). Most of the porphyry deposits exhibit a well-developed zonal pattern of mineralization and wall-rock alteration that can be defined by broad variation in major oxide and trace element concentration.

As a result these deposits are suitable targets for application of lithogeochemical techniques for exploration (Atapour and Aftabi, 2007).

The mineralization at Darrehzar is associated with a granodiorite stock intruded into thrusted and folded early Tertiary volcano-sedimentary series comprising and andesitic lava, tuffs, ignimbrites and agglomerates.

The alteration at Darrehzar consist a potassic zone which is characterized by K-feldspar+quartz±chalcopyrite. This potassic zone has been overprinted by a retrograde phyllic alteration.

In this study for the first time, geochemical evolution of Darrehzar granodiorite rocks as a possible indication of porphyry Cu-Mo-Au mineralization is documented. Also in this research, the mass changes of major and minor elements that accompanied alteration in granodioritic rocks of the Darrehzar porphyry copper deposit is evaluated quantitatively and the hydrothermal alteration episodes are studied in terms of mass transfer and element mobility. These changes are illustrated quantitatively by isocon plots.

Corresponding Author: Reza Derakhshani, Department of Geology, Shahid Bahonar University, Kerman, Iran
Tel: +989131411496 Fax: +983412510643

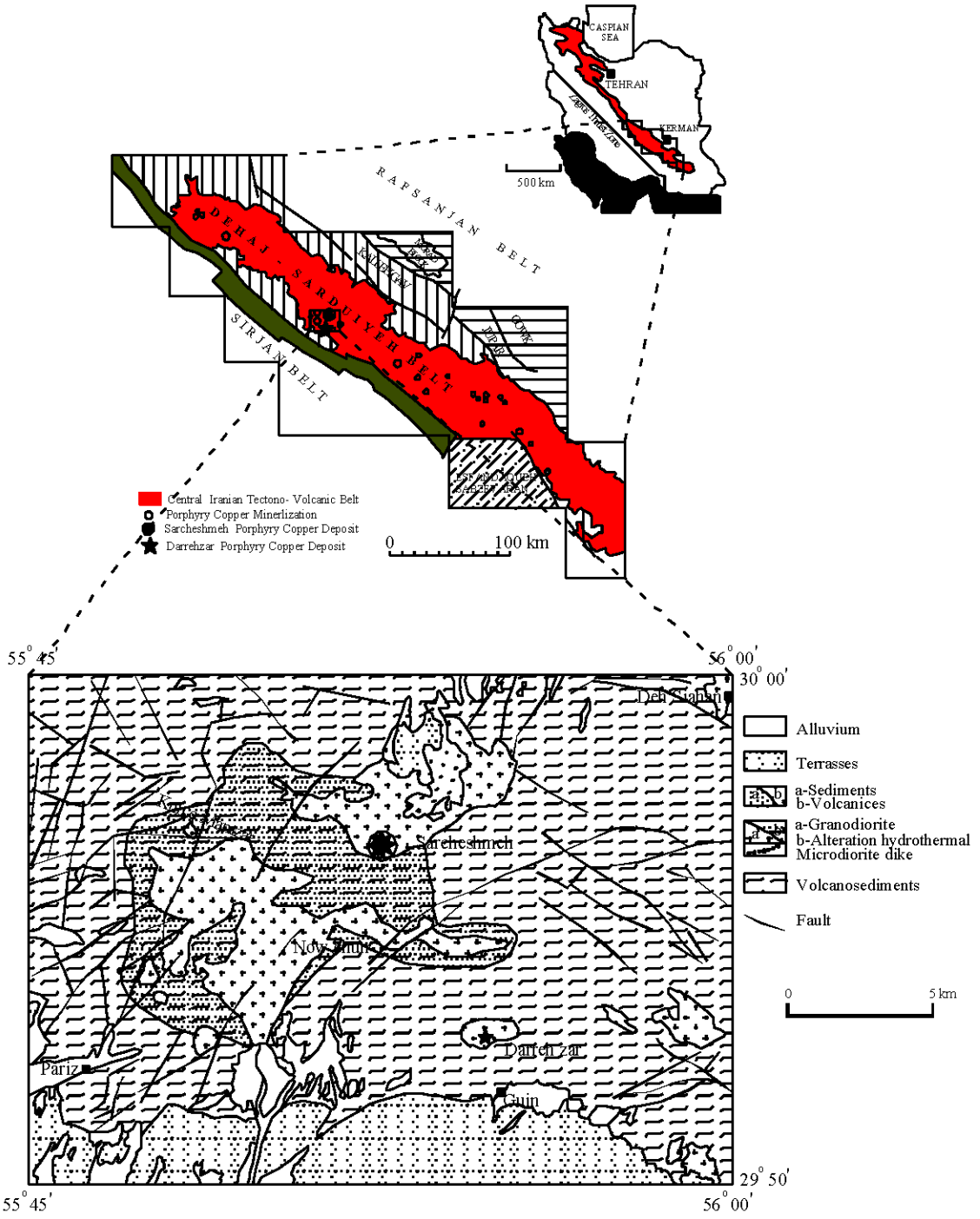

Fig. 1: Sketch map showing the position of the Central Iranian Tectono-Volcanic Belt and Porphyry- type Cu deposits, Sub-parallel to the Zagros Thrust zone and generalized geologic map of study area. Darrehzar and Sarcheshmeh porphyry deposits that are of the most important Cu deposits of Iran, located in the Central Iranian Tectono-Volcanic Belt

The masses of components added to or removed from the rock as a result of its interaction with hydrothermal fluids are determined by comparing the corrected analyses for the altered rocks with those of least-altered equivalents.

MATERIALS AND METHODS

This study which is conducted in 2007 is concentrated on alteration zoning in the porphyry copper deposit of Darrehzar, Iran. Elements that are immobile during hydrothermal alteration and other interactive water-rock systems are concentrated during net mass loss and diluted by net mass gain. Calculations of these changes (material changes) requires different approaches when the altered rocks are derived from one, or more parent rock (single or multiple precursor). In single precursor systems the changes are calculated as displacements from a uniform rock composition.

In this system, residual concentration and dilution of immobile elements produce linear arrays of data on binary diagrams that contain the precursor composition and extrapolate to the origin. Element having chemical affinity must be avoided in such tests because of unaltered correlation. Mass changes are calculated from the concentration ratio of an immobile element in an altered samples and its precursor. The method of mass changes was used to show that Al, Ti, Zr, Ga and Y were highly immobile in the alteration zone of Darrehzar copper porphyry. They have shown that Al and Ti were extremely immobile during hydrothermal alteration of intrusive rocks.

The best fit line to binary plot of magmatic incompatible elements passes through the origin. If these elements are immobile during alteration, addition of other material (as in silicification) dilutes their concentration and they plot closer to the origin, whereas extraction of material (as by solution) concentrates them and they plot farther away from the origin.

GEOLOGY OF DARREHZAR AREA

Darrehzar is located 8 km Southeast of the Sarcheshmeh porphyry Cu deposit in Southwest of Iran. The topography around the deposit is mountainous with altitudes ranging from 2375-2595 m. The surrounding area is composed of Eocene volcano-sedimentary complex which is invaded by intrusive rocks and overlaid by Neogene sediments. They crop out as small stocks of irregular shape. Mainly, it is granodiorite. These alterations are better developed in the western part of the area, while to the South the rock are less altered.

The central part of Darrehzar area is composed of intensively hydrothermal altered rocks (Ranjbar *et al*., 2001) covering the surface of about 1.8 km^2. Altered zone is elongated in Eastwest direction, while longer axis is about 2 km long, the shorter is 700-1000 m. Boundary between the altered and unaltered rocks is quite sharp and clear, but in some parts it is very irregular. The fresh rocks are sometimes embraced by the altered ones.

Hydrothermal alteration is very intensive. In addition the weathering changed them even more, so that, even in thin sections it is often impossible to determine the kind of rock. Granodiorite porphyry is situated in the central part of alteration zone.

The Darrehzar is a granodiorite pluton of Oligocene-Miocene that intrudes Eocene volcanic sedimentary complex comprised mainly of volcano-classtic, andesite, trachyandesite and sedimentary rocks (Fig. 2).

Dykes of quartz-microdiorite, microdiorite and granodiorite intrude the volcanic sedimentary complex in the Southern part of area (Derakhshani and Abdolzadeh, 2009).

The hydrothermal altered rocks are high fractured and supergene alteration has produced extensive limonite and leaching of sulfide, giving a characteristic reddish or yellowish color to the altered rocks. Weathered zone developed up to 80 m below the surface. This weathering resulted in a supergene enriched zone with an average thickness 34 m and average grade of 0.8% Cu. The hypogene zone, in the central and the peripherally part of the deposit averages 0.3% Cu and 0.1% Cu, respectively.

Chalcopyrite is the most abundant primary Cu-bearing mineral. In the supergene zone, chalcocite is abundant and covellite is rare. Pyrite is present throughout the deposit as impregnations and veinlet in the matrix of the altered rocks.

Surface and subsurface samples of the hydrothermal alteration rocks indicated intense alteration involving chlorite, albite, epidote, quartz, sericite, biotite and clay minerals. Propylitic and phyllic alterations are pervasive in the surface rocks with sporadic small area of argillic alteration. However, argillic alteration is difficult to distinguish from supergene weathering of the primary alteration type; in order to improve resolution of such areas, integration of remote sensing and geophysical data may be helpful (Honarmand *et al*., 2002).

The area surrounding the Darrehzar porphyry copper deposit consists of upper Eocene volcanics (Amidi *et al*., 1984) and sediments intruded by Miocene granodiorite porphyry and equivalent dykes, covered partly by Quaternary deposits.

The volcanics, pyroclastic and sediments are the oldest rocks in Darrehzar area. The lower part of volcanic

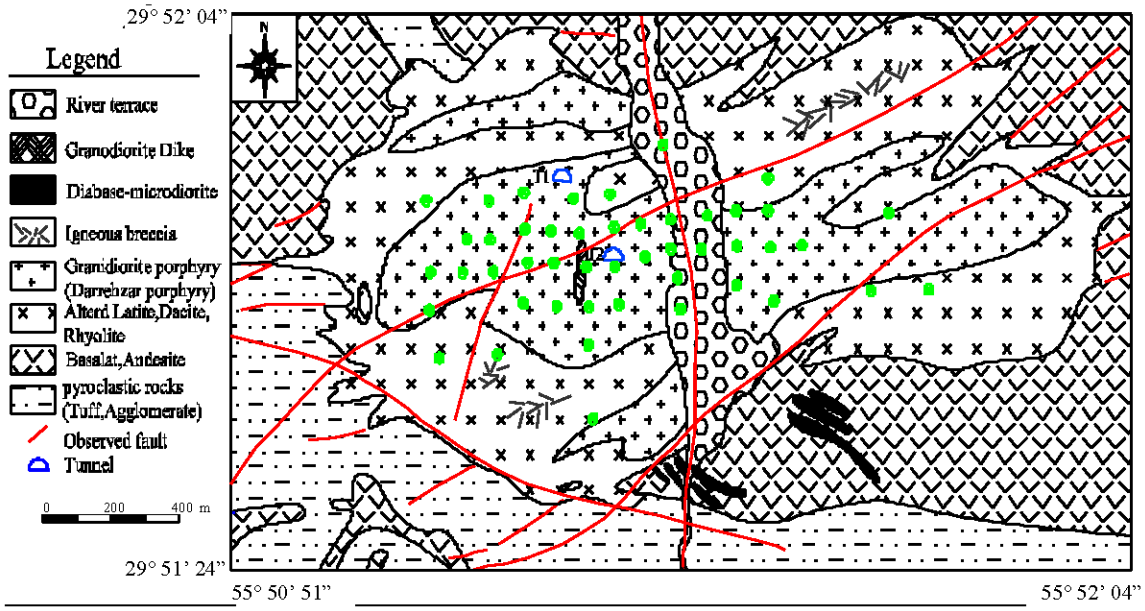

Fig. 2: Detailed Geologic map of the Darrehzar area. Distribution of some igneous rocks such as granodiorite, andesite, rhyolite, andesite, diabase microdiorite and also some pyroclastic rocks, tuff and agglomerate is shown in this map. Also major faults of the study area are mapped

sedimentary complex consists of trachyandesite flows and upper part mainly of pyroclastics and sediments.

Trachyandesite forms masses in the Northern, Northeastern and Southeastern part of the explored area and relatively thin lava flows in the pyroclastic sequence in the Southern and Southwestern part of the area. The rock is mostly compact magnetite is very common accessory mineral.

Pyroclastics and sediments are predominant in the south consisting of agglomerate, tuff, conglomerate, sandstone and limestone. Locally, the agglomerates are altered, mostly chloritized and hematitized.

The intrusive rocks (granodiorite) crop out mainly in the central part of Darrehzar area. The main intrusive body outcrop is about 2 km long and 100-500 m wide oriented Eastwest and dipping 60-80° to the North.

The volcanic-sedimentary complex as well as the granodiorite porphyry intrusive has been strongly faulted. In generally the complex strikes West-northwest and dips South-southwest at 10-40°. The most important faulted strike East or East-northeast. Intrusion probably took place along a deep East-strike fault. Subsequent faulting has been strong, causing intensive fracturing and shearing of both the intrusive and the surrounding volcanites.

Hornblende, produced by contact metamorphism has been found locally in the Southern part of area and at a few places in the north also. Very intensive alterations have been taken place in the intrusives and also in the surrounding rocks. The surface of the altered area is almost 5 times lager than that of the outcrop of the intrusion.

An oxidation zone is well developed and large masses of limestone are present within the altered zone. In places, sulfide mineralization crop out, as in the valley of Rud-e-Darrehzar.

The primary mineralization (hypogene porphyry copper) is generally low (0.3% or less) but between 0.4 and 0.5% in the deeper drill holes in the central part of the explored area, the secondarily enriched zone is well developed in the central part of the explored area, where the oxidation and leaching of the capping was most intensive. The capping is from several meters up to 100 m thick. The copper ore body with average ore grade 0.46% (cut-off grade 0.4%) contains about 50,000,000 tons of ore. The ore body contour encloses an area of 0.3 km^2.

PETROGRAPHY

Darrehzar stock: The Darrehzar stock is a complex intrusive body, which crop out over an area of about 1 by 2.2 km. This stock consists of granodiorite composition. It is not possible to find completely fresh rock in the Darrehzar stock. Petrographic observations in thin sections indicate that granodiorite rock contains 50-65 volume percent phenocrysts including mainly zonal

plagioclase, highly altered hornblende, quartz and biotite. Hornblende was the earliest major mineral for crystallization and forming euhedral to subhedral phenocrysts. Quartz phenocrysts crystallized after them, ubiquitously rounded or embayed. Plagioclase phenocrysts (mainly subhedral) formed shortly after the quartz phenocrysts and biotite phenocrysts (subhedral to anhedral) formed late. The granodiorite groundmass is fine grained and consists mainly of quartz, plagioclase and K-feldspar, with lesser biotite and amphibole. Apatite, zircon, titanite and rutile are present in minor to trace element.

Dykes consist mainly of plagioclase, K-feldspar, biotite, quartz and highly altered amphibole. Plagioclase occurs both as microcrystals in the groundmass and phenocrysts and composes more than 40% of the total volume of the rock unit. K-feldspar crystals compose up to 30 vol. percent of the total volume of the rock and occur both as phenocrysts and in the groundmass. Apatite, quartz and magnetite occur as inclusion in the plagioclase and K-feldspar.

The phenocryst assemblage in the Darrehzar granodiorite porphyry consist of quartz, hornblende, biotite, plagioclase (andesine-oligoclase), K-feldspar with accessory magnetite, zircon, apatite and sphene, similar to that of, I-type or magnetite series granites.

In thin sections, these rocks are characterized by abundant phenocrysts of quartz and feldspar and lesser mafic mineral (chloritic pseudomorphs biotite or hornblende). Feldspars are extensively sassuritized, but relict plagioclase twinning can be observed locally. Quartz phenocrysts frequently show deep embayments.

Andesite is typically green-gray to brown-gray, holocrystalline and porphyritic with a fine grained matrix. It consists of essential plagioclase, orthoclase, blue-green to brown hornblende, magnetite and trace amounts of biotite, clinopyroxene, quartz, rutile, apatite and zircon.

Andesitic volcanic rocks: Extrusive rocks of the Darrehzar volcanic complex consist dominantly of pyroclastic breccias with minor interlayered massive or lava flows, Amphibole-plagioclase andesites prevail, but the total compositional range extends from basalts±clinopyroxene phenocrysts. Composition and phenocrystic variations within the intrusions indicate one or several cycles of magmatic differentiation by crystal fractionation.

ALTERATION AND MINERALIZATION

Hydrothermal alteration and mineralization at Darrehzar are centered on the stock and were broadly synchronous with it emplacement (Fig. 3). Early Hydrothermal alteration was dominantly potassic and propylitic and was followed by later phyllic, silicic and argillic alteration.

Potassic alteration: The primary and secondary alterations in granodiorite stock are represented by potassic mineral assemblages developed pervasively and halos around veins in the deep and central part of the Darrehzar stock and mineral assemblages secondary in around stock.

The earliest alteration is represented by potassic mineral assemblages developed pervasively and as halos

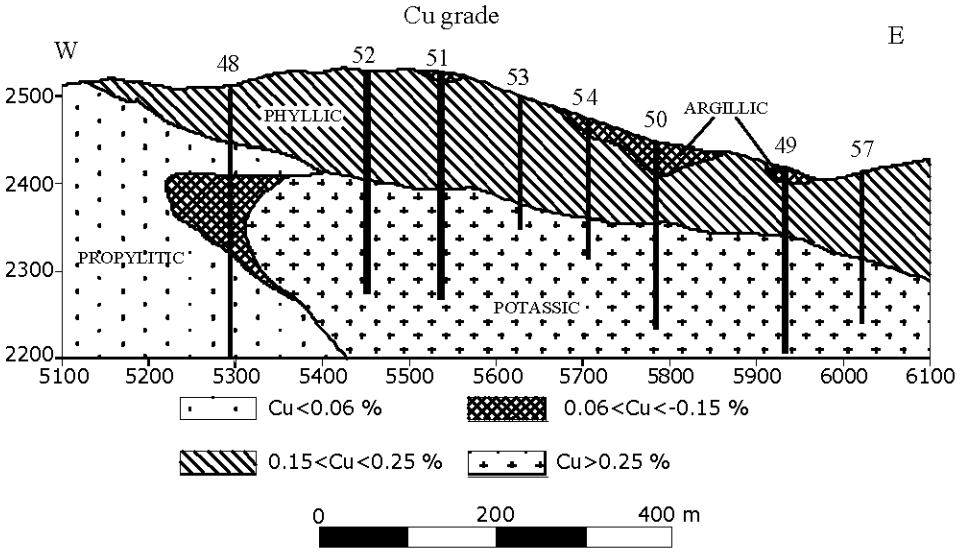

Fig. 3: Ore grade distribution along W-E section in Darrehzar area. The Cu ore grade distribution show similar pattern and define a high grade ore in potassic zone. Cu ore grade distribution in propylitic zone is less than 0.06% in argilic zone is between 0.06-0.15%, in phylic is between 0.15-0.25% and potassic zone is more than 0.25%

around veins in the deep and central part of the Darrehzar stock (Fig. 3). Potassic alteration is characterized by K-feldspar irregularly shape crystals of enriched biotite and anhydrite potassically altered rocks contain plagioclase, K-feldspar, ferromagnesian minerals (mainly biotite and sericite and chlorite) and chalcopyrite, pyrite, titanite, zircon and rutile.

There are two methods to distinguish differences of the potassic alteration: Potassic alteration in altered rocks is characterized by relict plagioclase with secondary biotite occurring in the matrix and replacing hornblende and less commonly magmatic biotite. Strong potassic contains secondary K- feldspar in the matrix and in plagioclase site, giving the rocks a pinkish appearance and shreddy biotite completely replaces mafic minerals. Magnetite in the potassic alteration is common with K-feldspar, quartz, biotite, chalcopyrite, occurring in veinlets, disseminated in the matrix and at sites of former hornblende due to breakdown to secondary biotite and magnetite. Primary minerals show zones replace large part of plagioclase and sometimes associated with white micas composition.

Igneous biotite is replaced by secondary biotite which crystallizes in small subhedral flakes. This replacement is frequently located at the rims of igneous biotite it can sometimes be complete in strongly altered samples some igneous biotite do not show those recrystallization features, but the presence of rutile between their cleavages and their chemistry indicate that they were affected by the potassic alteration.

Propylitic alteration: There is a relatively sharp boundary between the propylitic and potassic alteration zones in the deep part of the deposit. Propylitic alteration is pervasive and represented mainly by chloritization of primary and secondary biotite and groundmass material in rock peripheral to the central potassic zone. Epidote replaced plagioclase. Minor minerals associated with propylitic alteration are calcite, sericite and pyrite. The propylitic zone occurs in the peripheral parts of the system. Propylitic alteration is irregular in intensity and generally diffuses, except for some rare small epidote veinlets. The zone propylitic alteration surrounds the area of potassic alteration.

The most intense propylitic alteration is characterized by mineral assemblages with abundant epidote. Epidote and calcite were only rarely observed in the same sample, whereas calcite and chlorite occur together with propylitic alteration but partly overprint weak potassic alteration at the inner edge of the chlorite-epidote zone.

These types of rocks are generally pale green in color, which is due to the abundance of actinolite and chlorite.

Phyllic alteration: Phyillic alteration is characterized by the replacement of almost all rock-forming silicates by sericite and quartz and overprints the earlier formed potassic zone. Pyrite forms occur in veins and in the other hand, dissemination quartz veins are surrounded by chalcopyrite. Slicification was synchronous with phyllic alteration.

Argillic alteration: Feldspar is locally altered to clay down to a depth of 300 or 400 m, within 80 m of the erosional surface the entire rock has been altered to an assemblage of clay minerals, hematite and quartz. The affected rocks are soft and white colored.

The argillic alteration zone is characterized in shallow levels of the system, where it forms a blanket over the intrusion and replaces the phyllic zone downward and the propylitic fringe laterally. The alteration is manifested by an advanced replacement of plagioclase and mafic phase by clay mineral (XRD analyses indicate that mainly kaolinite, montmorillonite and illite, sericite and quartz).

Minealization: Hypogene copper mineralization was introduced during potassic and to a lesser extent during phyllic alteration and exists as disseminations and in veinlet form. During potassic alteration, the copper was deposited as chalcopyrite and minor bornite, later hypogene copper was deposited mainly as chalcopyrite hypogene molybdenite was concentrated mainly in the deep part of the stock and is associated exclusively with potassic alteration, where it is found in quartz veins accompanied by K-feldspar, anhydrite, sericite and lesser chalcopyrite. The concentration of sulfides and copper mineralization increase outward from the central part of the stock, with the latter generally reaching a maximum along the interface between the potassic and phyllic alteration zones and in silicified phyllically altered rocks. Sulfide concentration, mainly pyrite, is highest in the phyllic alteration zone.

At the exposed surface of the deposit, rocks are highly altered and the only mineral which has survived supergene argillization is quartz. Most of the sulfide minerals have been leached and copper was concentrated in an underlying supergene zone by downward-percolating groundwater. This zone is very limited and consists of a thin (up to 35 m) blanket containing covellite, chalcocite and digenite located below a thin, intensely oxidized cap.

The main Cu mineral in the deposit is chalcopyrite, which occurs as center line filling in quartz veins or patches between the quartz and magnetite grains of vein, i.e., petrographically late compared to the most of the veins. These veins are more commonly associated with biotite-K-feldspar-quartz alteration, with very narrow alteration halos of K-feldspar. Chalcopyrite is found also

disseminated in the potassic alteration and in parts of the quartz-magnetite veinlet where it is intergrown with magnetite or lies along grain boundaries between magnetite and quartz grains. Copper mineralization mainly situated in the hydrothermally altered granodiorite porphyrite rocks.

Mineralization in the Darrehzar occurs in two forms. The first form is fracture controlled and is spatially related to the quartz-feldspar porphyry. Vein mineralogy in this form is simple and consists mainly of quartz, chalcopyrite, galena and sphalerite. Pyrite and chalcopyrite are the most widely distributed in the vicinity of the fractures. Other minerals include minor amount of molybdenite and the gangue minerals are quartz, calcite, sericite and epidote.

The second mode of sulfide mineralization is in the form of disseminated pyrite in the pyrite-quartz –feldspar porphyry. Pyrite occurs as light yellow crystals exhibiting two distinct zones. Some pyrite crystals are surrounded by iron hydroxide rim which is formed by sequent supergene alteration and some contain sieved inclusions of chalcopyrite.

The intrusive bodies exhibit strong hydrothermal alteration which forms concentric zones, extending outward from the inner part of the intrusion like Sracheshmeh (Hezarkhani 2006a, b). These zones vary from a potassic core to a propylitic fringe through a well-developed annular feature of phyllic alteration and an irregularly developed argillic zone. The mineralization is present in two forms: disseminated and as stock work veins. Sulfide are disseminated in to the rock, chalcopyrite is common and is associated with secondary biotites or orthoclase, molybdenites most abundant sulfide mineral in Darrehzar.

Mineral composition and genesis: The stock has been intruded along east-west oriented fault system. Before the penetration of the hydrothermal solutions, the magmatic stock and the surrounding rock have been crushed. The numerous fissures pave the way to the alteration and penetration of mineralized solutions.

Pyrite occurs as veinlets and impregnations. Veinlets are generally very thin and pyrite only occasionally occurs in veins of 5-6 cm thick.

The enrichment of copper started much later, when the ore body was under the influence of exogenous conditions and the leaching of copper minerals took place in the oxidation zone and enrichment in the cementation zone. Only locally, due to the presence of carbonates, in inter-reaction with certain acids copper carbonates were created in the oxidation zone.

Supergene alteration: Two distinct supergene alteration zones recognized at Darrehzar: 1-Oxidized and leached zone and 2-supergene sulfide zone.

The mineral assemblages' characteristics of the oxidized and leached zone are kaolinite, Fe-oxides and Hydroxides (goethite, limonite and hematite), sulfate (jarosite) and carbonates (malachite and Azurite).

The supergene sulfide such as covellite, chalcocite and minor amounts of bornite, along with lesser amounts of native copper and cuprites could be found at the top of the zone. The main copper mineral in the enrichment zone is chalcocite. During the process of enrichment the copper sulphates migrated downwards. Due to the change of pH value (acidity diminished) and lack of oxygen near the under groundwater table the solutions turned in to neutral or alkaline and copper precipitated as chalcocite. Chalcocite occurs as small grains, veinlets along the fissures and also as thin coatings around the pyrite and chalcopyrite minerals. For the enrichment the grade of primary ore was very important. Although in the whole area the conditions for enrichment have been favorable, the content of copper in the enriched zone was higher only in the central part of the altered zone (granodiorite porphyry). It may be explained by the fact that the primary mineralizations in the central part contain an average of 0.28% of copper, while the peripheral parts contain only 0.09%.

GEOCHEMISTRY

The chemical composition of each altered rock was compared to that of an unaltered igneous rock with similar SiO_2 content. Several chemical changes related to hydrothermal alteration can be recognized. One of the problems in determining the magmatic differentiation history of a porphyry copper system is that most of the rocks exposed exhibit varying degree of alteration that affect the major and trace element compositions The unaltered andesites are metaluminous and alkaline; the unaltered granodiorites are metaluminous to peraluminous and subalkaline. To linear variation in Na_2O+K_2O/SiO_2, V/TiO_2, SiO_2 vs TiO_2 and SiO_2 vs. Zr/TiO_2 and various major elements suggests that the igneous rocks are comagmatic. Pearce element plots of Na/Zr vs. Al/Zr and (K+Na)/Mg vs. Al/Mg indicate that magmatic differentiation was controlled in part by feldspar fractionation. The igneous rocks are classified as syn-collusion to volcanic arc granite. This data are consistent with highly evolved arc magmatism related to subduction of neo-thetis oceanic plate regarding to Arabia-Eurasia collision (Talebian and Jackson, 2002; Rahnama Rad *et al.*, 2008). Collectively, these data suggest that the igneous rocks are part of a differentiated comagmatic suite. The composition of the altered rocks is consistent with alteration mineral assemblages and reflects the dominance of potassic alteration.

Mass change calculations methods: In this part of study the technique used for calculation of mass changes is the one that was presented by the isocon method of Grant (1986) and the immobile element method of Maclean (1988). The method is based on elements that have not been affected by alteration, that is, elements that can be shown to have been highly immobile. Major and trace elements which have been demonstrated to be immobile during hydrothermal alteration at other deposits, Al, Ti, Zr, Ga, Y, Nb and REE (Yb, Lu), are suitable for this purpose. This elements are concentrated in rocks when mass is lost (as by solution) and on binary diagrams they plot farther away from the origin than those the parent rock (precursor). In the case of mass gain by addition of other materials (as by silicification), the immobile elements are diluted and plot close to the origin. The mass change calculations are similar to those of and Grant (1986), but neither of these studies is based on immobile elements.

The first step in identifying precursor rock compositions and calculating mass changes is to choose the elements that were most immobile during the alteration. Pairs of the elements are plotted on binary diagrams and correlation coefficients for regression lines are calculated. Regression lines that pass through the precursor composition and origin indicate that the element were the immobile or at least did not move out of the alteration system. Element pairs that have the highest correlation coefficients indicate the least mobility and are used as the most immobile elements. Sample are used must be of the same affinity (e.g. tholeitic, calc-alkaline) because different affinities have different concentration ratios of immobile elements.

Single precursor method: Mass and chemical changes can be calculated from changes in concentration of immobile elements when the altered samples are derived from a single parent rock. In binary plot diagrams, residual concentration and dilution of the immobile elements produce linear arrays of data that pass through bulk composition and the origin. Mass changes are calculated from the concentration ratio of an immobile element in an altered sample and its precursor using following equations, where F is Enrichment Factor and RC is Reconstructed Composition.

$$F = RC = \text{Altered Rock} * F$$

$$\text{Mass Changes} = RC - \text{Precursor Composition}$$

The least-altered granodiorite samples are typically found in the deepest part of the deposit. Two samples rocks were selected and compared in terms of element concentration. Most of elements plot close to or on these isocons, which illustrates a very similar composition of chosen precursor samples (Fig. 4, Table 1). Based on the latter sample (GD) was selected to represent the precursor (least-altered) rock for comparison with alteration zone rocks (five samples).

Mass changes during potassic alteration: Comparison of sample D36, representative of the potassic zone, with least-altered sample, GD, shows that the immobile elements, Ti, Al and Zr plot close to or on a line of constant mass with a slope of 1.0 (Fig. 5, Table 2). However, the elements Ga which is generally considered to be geochemically immobile, plot off the line, possibly due to a nugget effect.

As expected from the mineral assemblage in the potassic alteration zone, K and Ba are enriched in sample D36 and copper as expected, is strongly enriched. By contrast Na is depleted, as are Fe, Ca and Mn. The gains and losses of major and trace element for the selected samples pairs are shown graphically in Fig. 6.

Pair of least altered porphyry, sample GD and K-feldspar-biotite alteration, Fig. 6, indicate strong gain in K, Si, S, Ba and Cu and lose of Na, Ca, Sr during potassic alteration. During the consumption of hornblende and plagioclase Ca and probably Sr removed and Mg is essentially conserved in the replacement of chain silicates to biotite.

The large amounts of Ca that was probably removed from the potassic zone may contribute to the addition of calcite and epidote in the surrounding propylitic zone. Ti is assumed to be immobile and occurs as titanite in the unaltered as well as the altered samples.

Phyllic alteration: Phyllic alteration zone is characterized by presence of the large proportions of sericite and pyrite and absence of biotite and K-feldspar. Phyllic alteration has strongly overprinted earlier potassic alteration. Comparison of potassically altered sample, D36 and representative sample, D2, for phyllic alteration shows that the immobile elements Al and Ti plot close to or on a line (Fig. 7, Table 3) of constant mass with a slope of 1.0. However, Zr, which is typically immobile, plots of the line, possibly due to a nugget effect as discussed earlier. The most important mass changes in the phyllic alteration zone relative to potassically altered rock are strong depletion of Na and Ba moderate depletion of K, Fe and Rb and addition of Ca, Mg, Mn and addition of Ca, Mg, Mn and SiO_2 and Cu. The gains and losses of major and trace element for the selected samples are shown graphically in Fig. 8.

Comparison of sample D3 (sample phyllic) with least-altered sample (GD) showed in Fig. 9 and Table 4. Phyllic

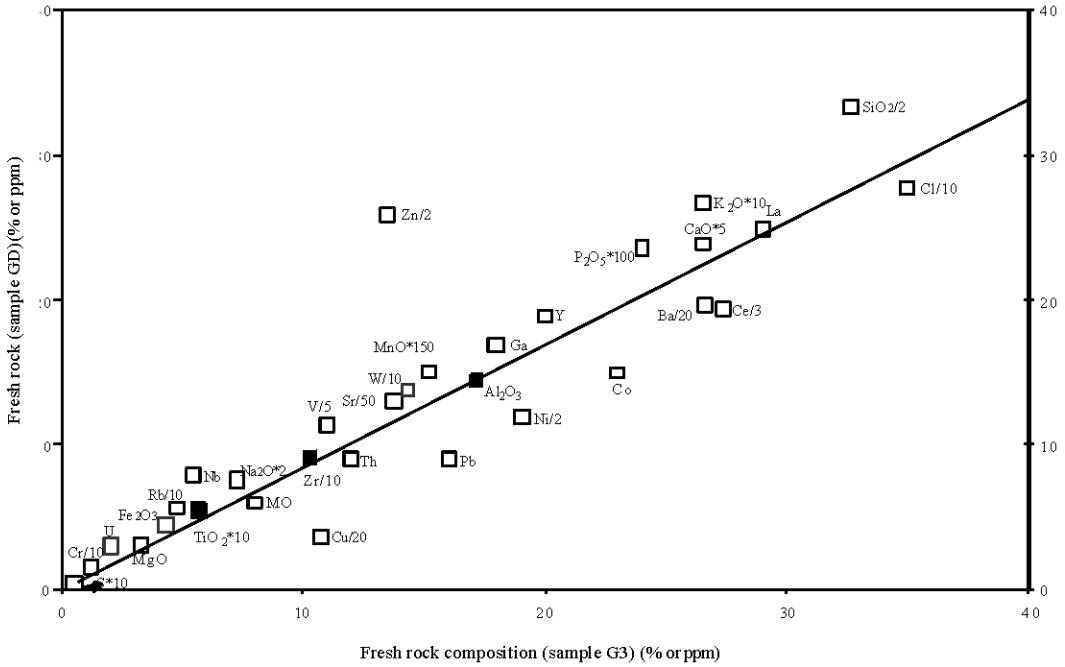

Fig. 4: Isocon diagram comparing two least-altered rocks. Almost all major oxides fall on or near a line with a slope. Black line (Isocons) is defined by the constant ratios of immobile element (Al_2O_3, TiO_2), which were used for the calculation of the gains and losses. Elements above this line are enriched in altered rock, whereas elements below the line are depleted during alteration. Oxides and S are in wt percent, and elements are in ppm unit

Table 1: Variations in major and trace element mass changes in the fresh rock

		Granodiorite fresh rocks				Major element normalized to 100% for mass changes calculations				
Sample	Units	G1	G2	G3	GD	G1	G2	G3	GD	Average
SiO_2	%	66.7	68.2	65.2	66.7	64.9	65.3	64.0	64.7	64.7
Al_2O_3	%	15.5	15.8	16.1	15.8	15.1	15.1	15.8	15.3	15.3
Fe_2O_3	%	4.9	4.5	4.3	4.6	4.8	4.3	4.2	4.4	4.4
CaO	%	4.3	4.7	5.3	4.8	4.2	4.5	5.2	4.6	4.6
Na_2O	%	3.4	4.3	3.6	3.8	3.4	4.1	3.5	3.7	3.7
MgO	%	3.5	2.9	3.2	3.2	3.4	2.8	3.1	3.1	3.1
K_2O	%	2.9	2.5	2.7	2.7	2.8	2.4	2.6	2.6	2.6
TiO_2	%	0.5	0.5	0.6	0.6	0.5	0.5	0.6	0.5	0.5
MnO	%	0.09	0.11	0.10	0.10	0.09	0.11	0.10	0.10	0.10
P_2O_5	%	0.22	0.25	0.24	0.24	0.21	0.24	0.24	0.23	0.23
S	%	0.05	0.04	0.05	0.05	0.05	0.04	0.05	0.05	0.05
Cl	ppm	278	113	350	278	278	113	350	247	247
Rb	ppm	57	62	48	57	57	62	48	55.66	55.7
Sr	ppm	650	720	685	650	650	720	685	685	685
V	ppm	57	48	55	57	57	48	55	99	64.75
W	ppm	138	141	143.5	138	138	141	143.5	140.83	140.8
Y	ppm	19	17	20	19	19	17	20	18.7	18.7
Zr	ppm	105	108	99	105	105	108	99	104	104
Zn	ppm	52	33	27	52	52	33	27	37.3	37.33
Mo	ppm	6	6	8	6	6	6	8	6.6	6.65
Ba	ppm	395	640	531	395	395	640	531	522	522
Ce	ppm	58	65	82	58	58	65	82	68.3	68.3
La	ppm	25	33	29	25	25	33	29	29	29
Ga	ppm	17	19	18	17	17	19	18	18	18
Co	ppm	15	19	23	15	15	19	23	19	19
Cr	ppm	15	6	12	15	15	6	12	11	11
Cu	ppm	72	95	214	72	72	95	214	127	127
Nb	ppm	8	13	5.4	8	8	13	5.4	8.8	8.8
Ni	ppm	24	29	38	24	24	29	38	30.3	30.3
Pb	ppm	9	14	16	9	9	14	16	13	13
U	ppm	3.1	2.4	2	3.1	3.1	2.4	2	2.5	2.5
Th	ppm	9	11	12	9	9	11	12	10.6	10.65

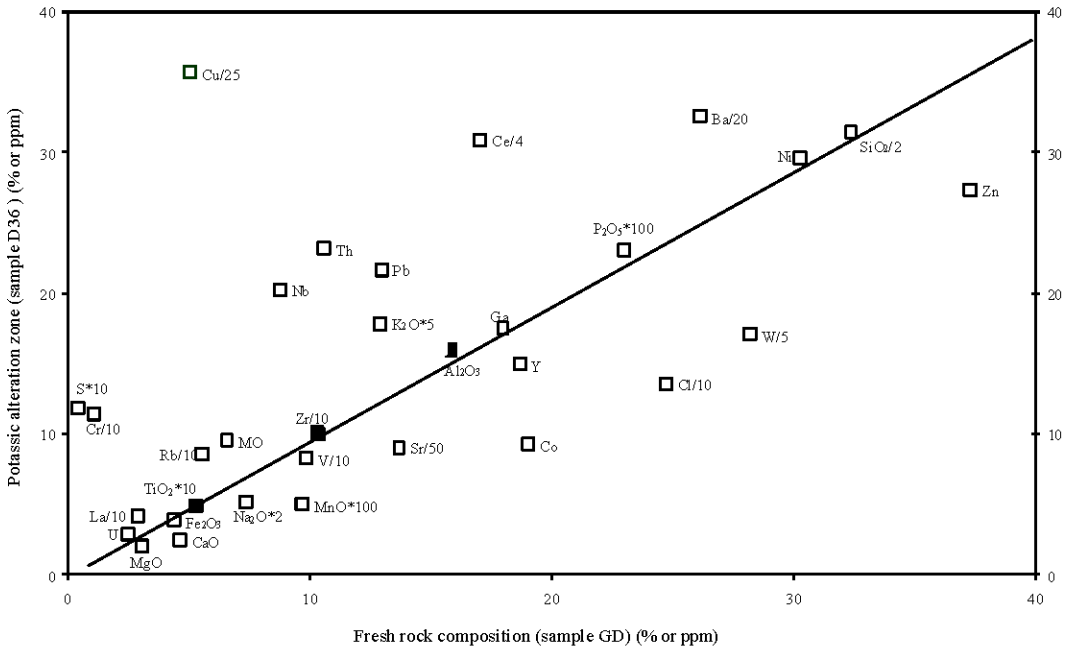

Fig. 5: Isocon diagrams with selected and weighted elements in which the fresh (least-altered, GD) versus the altered sample is plotted

Table 2: Major and trace element mass changes at the Darrehzar deposit in alteration potassic versus the least-altered sample (GD)

		Potassic alteration			Major element normalized to 100% for mass changes calculation			Mass changes in the potassic alteration zone			
Sample	Units	D34	D35	D36	D34	D35	D36	D34	D35	D36	Averege
SiO_2	%	59.8	61.4	62.8	65.5	65.1	65.8	1.7	13.3	3.6	6.2
Al_2O_3	%	15.6	16.3	16.3	17.1	17.2	17.1	2.0	5.3	2.4	3.3
Fe_2O_3	%	3.7	4.0	3.8	4.1	4.2	4.0	-0.3	0.6	-0.3	0.0
CaO	%	2.2	2.7	2.5	2.4	2.9	2.6	-2.2	-1.2	-2.0	-1.8
Na_2O	%	2.4	2.6	2.6	2.7	2.7	2.7	-1.0	-0.4	-0.9	-0.7
MgO	%	1.7	2.2	2.0	1.8	2.3	2.0	-1.3	-0.4	-1.0	-0.9
K_2O	%	3.1	3.4	3.6	3.4	3.6	3.7	0.9	1.8	1.3	1.3
TiO_2	%	0.48	0.42	0.49	0.52	0.44	0.51	0.00	0.00	0.00	0.00
MnO	%	0.04	0.05	0.05	0.04	0.05	0.05	-0.05	-0.03	-0.04	-0.04
P_2O_5	%	0.24	0.22	0.23	0.26	0.23	0.24	0.03	0.04	0.02	0.03
S	%	2.03	1.13	1.18	2.23	1.19	1.24	2.21	1.39	1.24	1.61
Cl	ppm	241.8	142.6	135.6	241.8	142.6	135.6	-1.71	-76.1	-106.1	-61.3
Rb	ppm	83.6	87.8	86.0	83.6	87.8	86.0	29.1	49.6	33.7	37.4
Sr	ppm	520	480	450	520	480	450	-126.3	-110	-145.7	-127
V	ppm	75.7	82.1	82.6	75.7	82.1	82.6	-22.2	-0.6	-13.2	-12
W	ppm	75.7	245	85.4	75.7	245	85.4	-64.1	152.7	-52.1	12.2
Y	ppm	17.61	15.7	14.9	17.61	15.7	14.9	-0.84	0.1	-3.2	-1.3
Zr	ppm	134	125.3	100.3	134	125.3	100.3	31.9	46.2	0.16	26.1
Zn	ppm	23.8	38.0	27.3	23.8	38.03	27.3	-13.2	8.3	-8.9	-4.6
Mo	ppm	8	7.3	9.5	8	7.3	9.5	1.51	2.14	3.26	2.3
Ba	ppm	986.6	1050.3	650	986.6	1050.3	650	478.6	736.6	153.1	456
Ce	ppm	79.65	85.6	123.6	79.7	85.6	123.65	12.5	34.3	60.1	35.62
La	ppm	23.76	24.84	41.5	23.76	24.84	41.5	-4.9	0.76	14.1	3.32
Ga	ppm	18.11	18.82	17.49	18.11	18.82	17.49	0.36	4.55	0.16	1.69
Co	ppm	22.03	4.91	9.2	22.03	4.91	9.2	3.34	-13.11	-9.44	-6.4
Cr	ppm	67.2	99.9	114.5	67.2	99.9	114.51	57.15	108.7	107.9	91.3
Cu	ppm	2196	879.2	891.7	2195.6	879.2	891.8	2100	926.6	799.1	1275.1
Nb	ppm	12.7	10.9	20.2	12.7	10.9	20.2	4.1	4.3	12.2	6.8
Ni	ppm	39.7	70.3	29.6	39.7	70.3	29.6	9.9	54.0	0.4	21.4
Pb	ppm	17.15	26.21	21.68	17.15	26.21	21.68	4.39	18.4	9.51	10.77
U	ppm	2.45	4.09	2.9	2.45	4.09	2.9	-0.01	2.4	0.51	0.96
Th	ppm	20.26	17.41	23.12	20.26	17.41	23.12	9.94	10.26	13.41	11.2

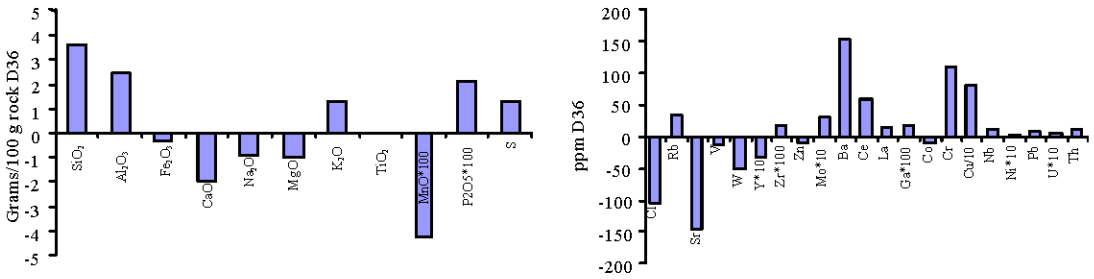

Fig. 6: Gains and losses of major and trace elements for alteration potassic versus the least-altered sample. Note the different scales of the diagrams

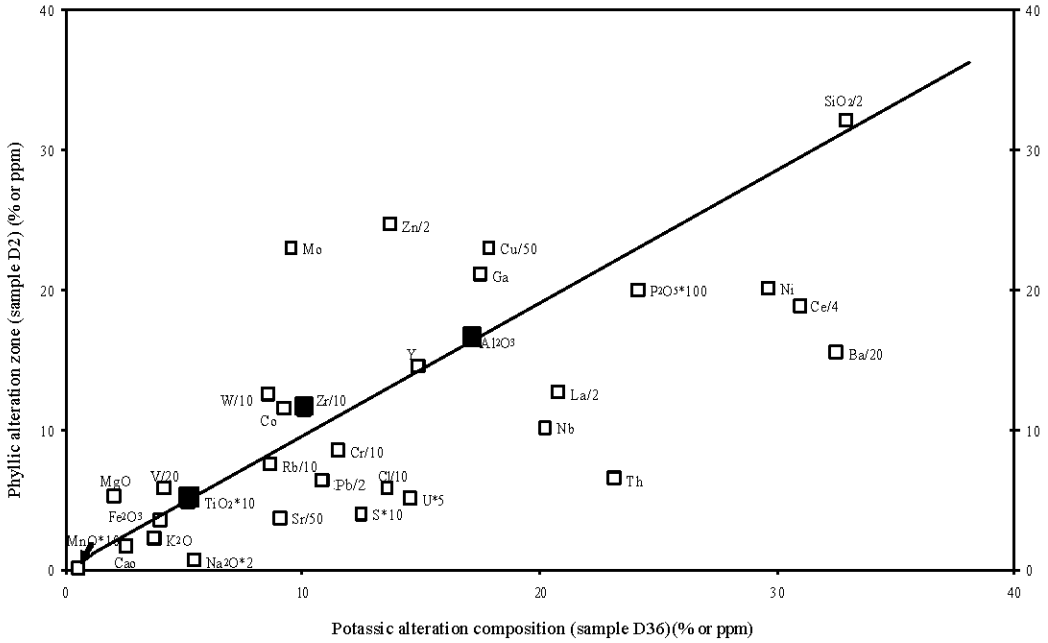

Fig. 7: Isocon diagram comparing the composition of a representative sample of an altered rock from the phyllic zone with that of a representative potassically altered rock

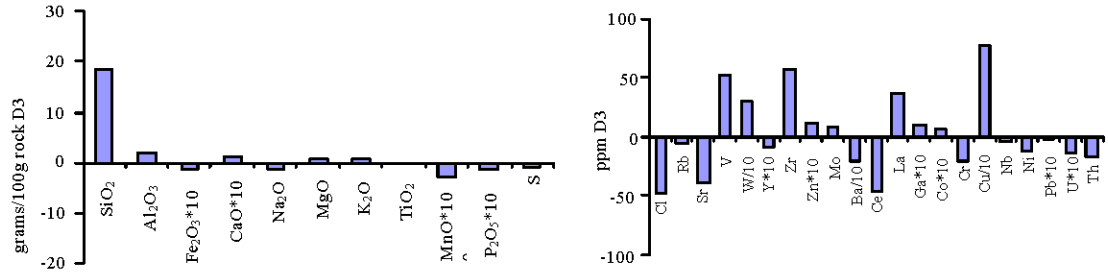

Fig. 8: Gains and losses of major and trace elements for alteration potassic versus alteration phyllic sample

Table 3: Major and trace element mass changes at the Darrehzar deposit in alteration potassic versus alteration phyllic sample

		Phyllic alteration			Major element normalized to 100% for mass changes calculation			Mass changes in the phyllic alteration zone			
Sample	Units	D1	D2	D3	D1	D2	D3	D1	D2	D3	Averege
SiO_2	%	70.4	64.3	72.3	73.6	68.1	70.3	3.7	3.0	18.6	8.5
Al_2O_3	%	15.2	16.3	16.3	15.9	17.3	15.9	-2.0	0.4	2.0	0.1
Fe_2O_3	%	3.2	3.5	3.3	3.3	3.7	3.2	-0.8	-0.2	-0.1	-0.4
CaO	%	1.5	1.6	2.3	1.6	1.7	2.2	-1.1	-0.9	0.1	-0.6
Na_2O	%	0.5	0.3	1.3	0.5	0.3	1.2	-2.3	-2.4	-1.3	-2.0
MgO	%	1.3	5.2	2.5	1.4	5.5	2.4	-0.8	3.6	0.9	1.2
K_2O	%	2.7	2.2	4.0	2.8	2.3	3.9	-1.1	-1.4	0.9	-0.6
TiO_2	%	0.52	0.48	0.44	0.54	0.5	0.42	0	0	0	0
MnO	%	0	0.01	0.02	0	0.01	0.01	-0.05	-0.04	-0.02	-0.04
P_2O_5	%	0.24	0.2	0.08	0.25	0.21	0.07	-0.004	-0.02	-0.14	-0.05
S	%	0.09	0.39	0.36	0.09	0.41	0.35	-1.15	-0.82	-0.82	-0.93
Cl	ppm	25.4	57.5	73.6	25.4	57.5	73.6	-111.6	-77.5	-47.3	-78.8
Rb	ppm	102.0	74.7	72.9	102.0	74.7	72.9	10.2	-10.5	1.5	0.42
Sr	ppm	194.09	184.5	342.0	194.1	184.5	342.0	-566.8	-563.5	-339.3	-490
V	ppm	65.3	116.3	112.3	65.3	116.3	112.3	-21.0	35.0	52.2	22.1
W	ppm	256	125	321	256	125	321	156.2	41.0	300	165.8
Y	ppm	12.65	14.45	11.69	12.65	14.45	11.69	-2.94	-0.28	-0.85	-1.36
Zr	ppm	112.3	113.8	131.5	112.3	113.8	131.5	5.8	14.7	57.6	26.0
Zn	ppm	29.61	49.2	32.2	29.61	49.2	32.2	0.63	22.4	11.4	11.5
Mo	ppm	5	23	15	5	23	15	-4.77	13.75	8.51	5.83
Ba	ppm	284	310	370	284	310	370	-381.9	-336.6	-205.6	-308
Ce	ppm	56.3	75.3	65	56.3	75.3	65	-70.5	-47.5	-45.6	-54.5
La	ppm	33.62	25.3	65.4	33.6	25.3	65.4	-9.8	-15.9	37.1	3.8
Ga	ppm	17.8	21.1	15.4	17.8	21.1	15.4	-0.7	3.8	1.0	1.4
Co	ppm	21.6	11.5	8.2	21.6	11.5	8.2	11.2	2.4	0.7	4.8
Cr	ppm	113.0	84.5	78.0	113.0	84.5	78.0	-7.8	-29.1	-20.9	-19.3
Cu	ppm	1250	1150	1385	1250	1150	1385	288.3	270.9	771.5	443.6
Nb	ppm	14.25	10.1	14.2	14.3	10.1	14.2	-6.8	-10.0	-3.1	-6.6
Ni	ppm	10.3	34.5	14.5	10.3	34.5	14.5	-19.9	5.3	-12.2	-9.0
Pb	ppm	15.3	12.8	17.83	15.3	12.8	17.83	-7.23	-8.73	-0.26	-5.41
U	ppm	5.25	1	1.2	5.25	1	1.2	2.05	-1.88	-1.45	-0.43
Th	ppm	5.06	6.5	4.74	5.06	6.5	4.74	-18.34	-16.55	-17.42	-17.4

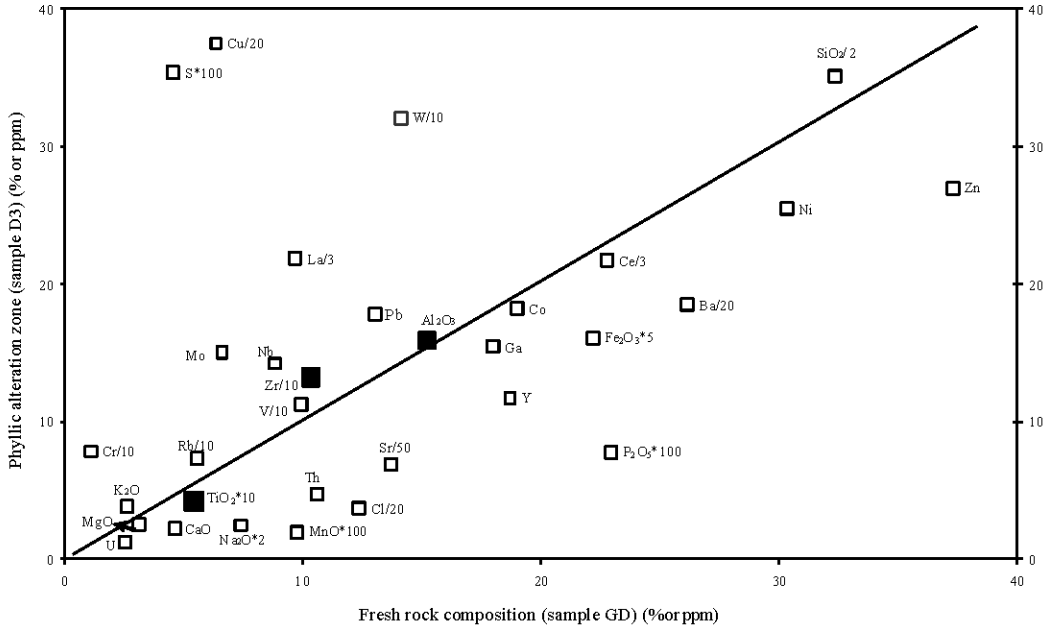

Fig. 9: Isocon diagram comparing the composition of a representative sample of an altered rock from the phyllic zone with that of a representative least-altered rock (GD)

Table 4: Major and trace element mass changes at the Darrehzar deposit in alteration phyllic versus the least-altered sample(GD)

		Phyllic alteration			Major element normalized to 100% changes calculation for mass			Mass changes in the phyllic alteration zone			
Sample	Units	D1	D2	D3	D1	D2	D3	D1	D2	D3	Averege
SiO_2	%	70.35	64.3	72.3	73.63	68.08	70.3	7.47	6.76	22.96	12.4
Al_2O_3	%	15.23	16.3	16.3	15.94	17.25	15.851	0.31	2.8	4.45	2.52
Fe_2O_3	%	3.2	3.5	3.3	3.34	3.7	3.2	-1.14	-0.53	-0.42	-0.7
CaO	%	1.5	1.56	2.3	1.57	1.65	2.23	-3.09	-2.9	-1.84	-2.61
Na_2O	%	0.46	0.3	1.25	0.48	0.31	1.21	-3.2	-3.34	-2.16	-2.9
MgO	%	1.3	5.23	2.51	1.36	5.53	2.44	-1.76	2.71	-0.05	0.3
K_2O	%	2.65	2.17	3.97	2.77	2.29	3.86	0.13	-0.17	2.23	0.73
TiO_2	%	0.52	0.48	0.44	0.54	0.5	0.42	0	0	0	0
MnO	%	0	0.01	0.02	0	0.01	0.01	-0.09	-0.086	-0.073	-0.083
P_2O_5	%	0.24	0.2	0.08	0.25	0.21	0.07	0.01	-0.007	-0.13	-0.04
S	%	0.088	0.393	0.363	0.09	0.41	0.35	0.04	0.39	0.39	0.27
Cl	ppm	25.41	57.47	73.56	25.41	57.47	73.56	-222.1	-186.7	-155.3	-188
Rb	ppm	102.0	74.72	72.9	102.0	74.72	72.9	44.3	22.79	35.26	34.12
Sr	ppm	194.1	184.5	342.0	194.1	184.5	342.0	-494.6	-491.2	-258.4	-415
V	ppm	65.3	116.3	112.3	65.3	116.3	112.3	-35.0	23.11	41.04	9.72
W	ppm	256	125	321	256	125	321	110.2	-9.57	259.5	120
Y	ppm	12.65	14.45	11.69	12.65	14.45	11.69	-6.29	-3.52	-4.11	-4.64
Zr	ppm	112.3	113.8	131.5	112.3	113.8	131.5	6.1	15.5	60.0	27.2
Zn	ppm	29.6	28	27	29.61	28	27	-8.3	-7.89	-3.62	-6.59
Mo	ppm	5	23	15	5	23	15	-1.69	17.55	12.1	9.32
Ba	ppm	284	310	370	284	310	370	-243.5	-196.5	-60.5	-166.8
Ce	ppm	56.3	75.3	65	56.3	75.3	65	-13.09	10.76	12.772	15.69
La	ppm	33.62	25.3	65.43	33.62	25.3	65.43	3.96	-2.43	52.6	18.04
Ga	ppm	17.8	21.1	15.4	17.8	21.1	15.4	-0.6	4.13	1.19	1.58
Co	ppm	21.6	11.5	18.2	21.6	11.5	18.2	2.2	-6.9	3.73	-0.33
Cr	ppm	113.0	84.5	78.0	113.0	84.5	78.0	99.8	77.8	86.2	87.9
Cu	ppm	720	890	750	720	890	750	578.9	807.5	808.4	731.6
Nb	ppm	14.25	10.1	14.23	14.25	10.1	14.23	5.17	1.8	8.94	5.3
Ni	ppm	21.1	34.49	25.47	21.1	34.49	25.47	-9.61	5.91	1.46	-0.75
Pb	ppm	15.3	12.8	17.83	15.3	12.8	17.83	2.001	0.44	9.23	3.89
U	ppm	5.25	1	1.2	5.25	1	1.2	2.64	-1.44	-1	0.06
Th	ppm	5.06	6.5	4.74	5.06	6.5	4.74	-5.63	-3.77	-4.68	-4.69

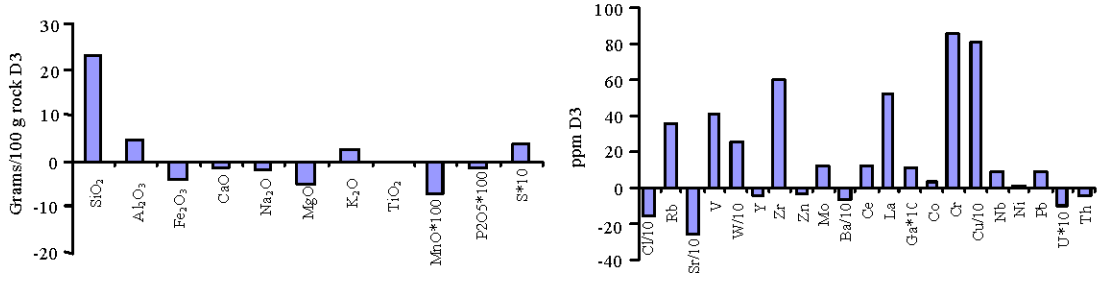

Fig. 10: Gains and losses of major and trace elements for alteration phyllic versus the least-altered sample

alteration generally leads to a loss Mg, Na, Ba and an addition Cu with some Pb, Rb and S. However, the same elements also depend on the amount of clay minerals, calcite and gypsum in the sample, respectively. The gains and losses of major and trace element for the selected samples pairs are shown graphically in Fig. 10.

Propylitic alteration zone: In general the propylitic alteration at the fringe of the deposit is characterized by enrichment in CO_2 and Ca some of which may have been directly transferred from the Ca-depleted potassic zone. However, the chlorite-epidote altered Darrehzar (sample D12) in comparison with least-altered sample (GD) only show a minor increase in Ca but is enriched in many other elements (Fig. 11, Table 5). Particularly Zn, Pb, Mn, Sr and Ba are enriched, where as Si and Rb are commonly depleted. The depletion in Na and K is due to the breakdown of plagioclase. The gains and losses of major and trace element for the selected samples pairs are shown graphically in Fig. 12.

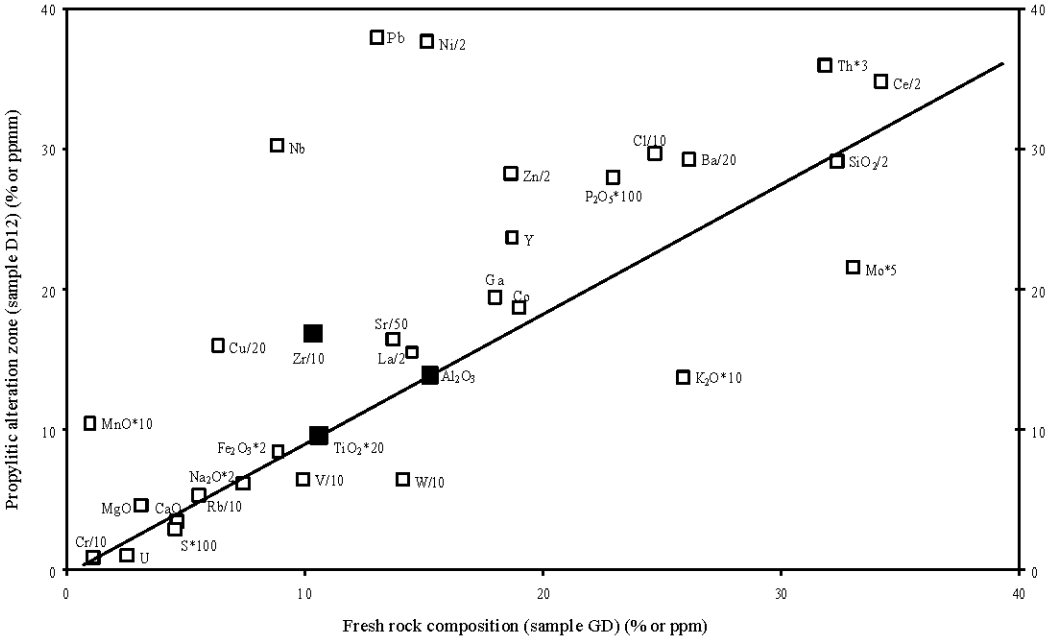

Fig. 11: Isocon diagram comparing the composition of a representative sample of an altered rock from the propylitic zone with that of a representative least- altered rock (GD)

Table 5: Major and trace element mass changes at the Darrehzar deposit in alteration propylitic versus the least-altered sample (GD)

		Propylitic alteration			Major element normalized to 100% changes calculation for mass			Mass changes in the propylitic alteration zone			
Sample	Units	D7	D8	D12	D7	D8	D12	D7	D8	D12	Averege
SiO_2	%	59.8	57.8	58.2	65.37	63.84	64.13	0.4	-4.24	-0.01	-1.28
Al_2O_3	%	13.7	14	13.9	14.97	15.46	15.31	-0.39	-0.66	0.13	-0.31
Fe_2O_3	%	3.8	4.1	4.2	4.15	4.52	4.62	-0.29	-0.14	0.23	-0.07
CaO	%	3.45	3.7	3.54	3.77	4.08	3.9	-0.88	-0.76	-0.7	-0.78
Na_2O	%	3.4	2.98	3.1	3.71	3.29	3.41	0.02	-0.56	-0.23	-0.26
MgO	%	3.49	3.45	4.6	3.81	3.81	5.06	0.7	0.51	2.01	1.07
K_2O	%	1.87	2.05	1.37	2.04	2.26	1.5	-0.54	-0.43	-1.06	-0.68
TiO_2	%	0.49	0.51	0.48	0.53	0.56	0.52	0	0	0	0
MnO	%	1.23	1.64	1.05	1.34	1.81	1.15	1.24	1.61	1.07	1.3
P_2O_5	%	0.22	0.25	0.28	0.24	0.27	0.3	0.009	0.03	0.08	0.04
S	%	0.028	0.045	0.029	0.03	0.04	0.03	-0.01	0.0019	-0.01	-0.01
Cl	ppm	320	410	297.46	320	410	297.46	71.81	141.3	53.12	88.74
Rb	ppm	55.84	53.13	52.76	55.84	53.13	52.76	-0.02	-5.33	-2.42	-2.59
Sr	ppm	750	780	820	750	780	820	62.23	53.86	142.34	86.14
V	ppm	60	70	65	60	70	65	-39.22	-32.69	-33.42	-35.11
W	ppm	45	49	64	45	49	64	-96	-94.41	-76.25	-88.9
Y	ppm	20.69	28.13	23.65	20.69	28.13	23.65	1.91	7.94	5.16	5
Zr	ppm	164.3	156.3	167.84	164.3	156.3	167.84	59.69	44.05	65.34	56.36
Zn	ppm	89.3	56.32	56.5	89.3	56.32	56.5	51.67	16.04	19.7	29.14
Mo	ppm	5.6	4.8	4.3	5.6	4.8	4.3	-1.02	-2.05	-2.26	-1.78
Ba	ppm	610.3	562.3	586.3	610.3	562.3	586.3	86.04	10.64	69.55	55.41
Ce	ppm	69.5	74.2	69.54	69.5	74.2	69.54	0.94	1.98	1.86	1.59
La	ppm	31.75	29.6	31.0	31.75	29.6	31.0	2.63	-0.96	2.29	1.32
Ga	ppm	17.7	18.25	19.45	17.7	18.25	19.45	-0.36	-0.71	1.62	0.183
Co	ppm	25.3	24.29	18.7	25.3	24.29	18.7	6.2	4.1	-0.13	3.39
Cr	ppm	12	13	9	12	13	9	0.9557	1.3144	-1.919	0.1169
Cu	ppm	250	420	320	250	420	320	122.1	270.8	195.8	196.2
Nb	ppm	23.2	24.1	30.2	23.2	24.1	30.2	14.31	14	21.67	16.66
Ni	ppm	98.2	65.3	75.32	98.2	65.3	75.32	67.53	31.55	45.69	48.26
Pb	ppm	16.35	25.3	37.94	16.35	25.3	37.94	3.28	10.96	25.28	13.17
U	ppm	2.3	1.2	1	2.3	1.2	1	-0.208	-1.36	-1.49	-1.02
Th	ppm	11	11.32	12	11	11.32	12	0.35	0.12	1.5	0.65

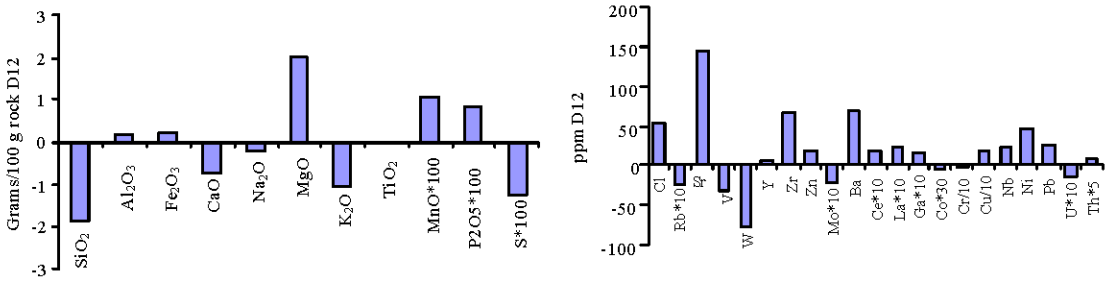

Fig. 12: Gains and losses of major and trace elements for alteration propylitic versus the least-altered sample

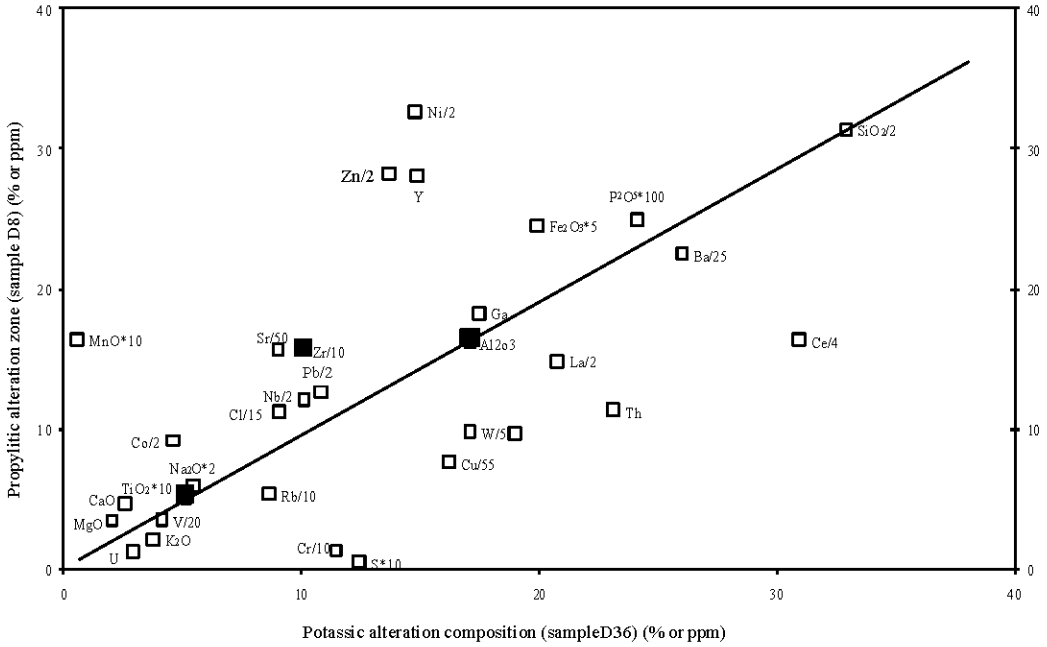

Fig. 13: Isocon diagram comparing the composition of a representative sample of an altered rock from the propylitic zone with that of a representative potassically altered rock

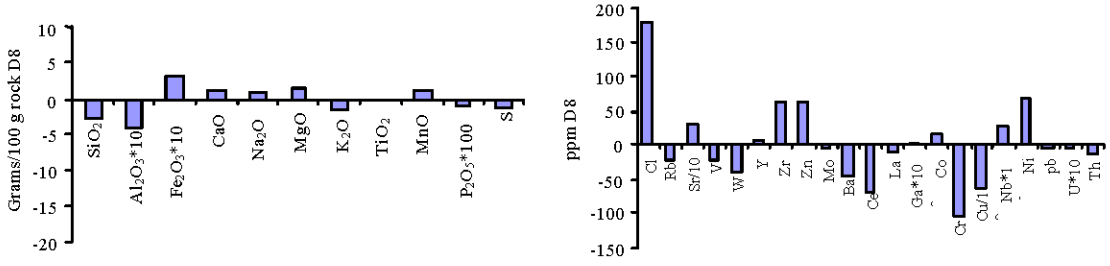

Fig. 14: Gains and losses of major and trace elements for alteration propylitic versus alteration potassic sample

Comparison of sample D36 (representative of the potassic zone) with propylitic sample (GD) showed in Fig. 13 and Table 6. Propylitic alteration generally leads to a loss K_2O, Na, Ba and some Rb and Ca, Mg, Zn and Mn are gained for this sample pair. However, the same elements also depend on the amount of clay minerals, calcite and gypsum in the sample, respectively. The gains and losses of major and trace element for the selected samples are shown graphically in Fig. 14.

Table 6: Major and trace element mass changes at the Darrehzar deposit in alteration potassic versus alteration propylitic sample

		Propylitic alteration			Major element normalized to 100% changes calculation for mass			Mass changes in the propylitic alteration zone			
Sample	Units	D7	D8	D12	D7	D8	D12	D7	D8	D12	Averege
SiO_2	%	60.2	62.7	63.1	63.78	63.06	63.05	-2.67	-2.63	1.74	-1.19
Al_2O_3	%	15.9	16.2	16.87	16.84	16.29	16.85	-0.4	-0.76	0.97	-0.06
Fe_2O_3	%	4.1	4.9	5.6	4.34	4.92	5.59	0.31	0.95	2.01	1.09
CaO	%	3.45	4.7	3.6	3.65	4.72	3.59	1.04	2.16	1.28	1.49
Na_2O	%	3.4	2.98	3.1	3.6	2.99	3.09	0.84	0.28	0.6	0.57
MgO	%	3.49	3.45	4.6	3.69	3.47	4.59	1.61	1.43	2.87	1.97
K_2O	%	1.87	2.05	1.37	1.98	2.06	1.36	-1.78	-1.67	-2.27	-1.91
TiO_2	%	0.49	0.51	0.48	0.51	0.51	0.47	0	0	0	0
MnO	%	1.23	1.64	1.05	1.3	1.64	1.04	1.23	1.6	1.07	1.3
P_2O_5	%	0.22	0.25	0.28	0.23	0.25	0.27	-0.01	0.01	0.05	0.01
S	%	0.0284	0.045	0.029	0.03	0.04	0.02	-1.21	-1.2	-1.21	-1.21
Cl	ppm	320	410	297.5	320	410	297.5	181.1	275.1	183	213.1
Rb	ppm	65.84	53.13	65.76	65.84	53.13	65.76	-20.86	-32.8	-15.57	-23.1
Sr	ppm	750	780	820	750	780	820	292.3	331.3	428.5	350.7
V	ppm	60	70	65	60	70	65	-23.25	-12.51	-12.99	-16.25
W	ppm	45	49	64	45	49	64	-40.86	-36.31	-16.83	-31.3
Y	ppm	20.69	28.13	23.65	20.69	28.13	23.65	5.58	13.29	10.44	9.77
Zr	ppm	164.3	156.3	167.84	164.3	156.3	167.84	62.31	56.27	79.52	66.03
Zn	ppm	89.3	56.32	36.5	89.3	56.32	36.5	61.06	29.1	11.78	33.98
Mo	ppm	5.6	4.8	4.3	5.6	4.8	4.3	-3.95	-4.69	-4.89	-4.51
Ba	ppm	610.3	562.3	586.3	610.3	562.3	586.3	-45.96	-86.7	-21.85	-51.5
Ce	ppm	56.3	65.3	59.3	56.3	65.3	59.3	-67.93	-58.23	-60.12	-62.1
La	ppm	31.75	29.6	31.0	31.75	29.6	31.0	-10.1	-11.85	-8.26	-10.1
Ga	ppm	17.7	18.25	19.45	17.7	18.25	19.45	0.02	0.79	3.35	1.38
Co	ppm	25.3	18.29	13.74	25.3	18.29	13.74	15.84	9.12	5.52	10.16
Cr	ppm	12	13	9	12	13	9	-103	-101	-105	-103
Cu	ppm	250	420	320	250	420	320	-644	-471	-549	-555
Nb	ppm	23.2	24.1	30.2	23.2	24.1	30.2	2.74	3.92	12.13	6.26
Ni	ppm	98.2	65.3	75.32	98.2	65.3	75.32	67.59	35.81	51.09	51.5
Pb	ppm	16.35	25.3	37.94	16.35	25.3	37.94	-5.49	3.66	18.96	5.71
U	ppm	2.3	1.2	1	2.3	1.2	1	-0.62	-1.69	-1.82	-1.38
Th	ppm	11	11.32	12	11	11.32	12	-12.2	-11.78	-10.3	-11.44

ELEMENTS BEHAVIOR AND ZONATION

Major and minor elements: Silicon was clearly added to both mine intrusive and wall rocks in the form of quartz vein. Expectedly, Si tends to be depleted in alteration types containing a high proportion of low Si mafic alteration products, increased in K-feldespar-rich assemblages due to the alteration of plagioclase.

Aluminum was fixed in a wide variety of alteration minerals and shows little overall variation. Iron released by silicated breakdown during K-silicate alteration was utilized in the essentially in situ formation of hydrothermal biotite, magnetite and sulfide minerals. However, particularly in the Darrehzar granodiorite, excess Fe released during biotitization processes migrated outward to the propylitic zone where it was fixed as pyrite (pyrite halo) and chlorite.

The Cu-Fe sulfides of the ore zone appear to have formed totally at the expense of Fe previously located in silicates and accessory oxides.

Copper and sulphur are generally increased in all alteration types but Cu/S ratios are markedly lower in propylitized and sites than in their bioitized equivalents.

Magnesium which was removed during propylitization of the Darrehzar granodiorite was apparently lost from the hydrothermal system, although some of that may have been added to areas of intensely biotitized and chloritized granodiorite and to retrograde alteration assemblages.

Calcium is strongly depleted in the K-silicate zone and the extent of this depletion decreased outward from the center of the ore body. The calcite and epidote formed by albitization of plagioclase and chloritization of mafic in the propylitic zone could not retain all the Ca that was liberated.

Mechanisms for Ca mobilization during potassic alteration are more divers (e.g., biotitization of hornblende or plagioclase alteration to K-feldspar or albite, amphiboltization of pyroxene) and relatively less of the liberated Ca was fixed in the K-silicate zone, although some was re-deposited as vein anhydrite within the intrusives. It is likely that much of the Ca was lost entirely from the hydrothermal system (as presently exposed) because Ca values only reach background levels in the outer part of the propylitic zone and there is no evidence to suggest that this element is

concentrated in rock either within or beyond this zone (Ca was also leached during retrograde) alteration processes.

Sodium lost during granodiorite alteration and also had been removed from hydrothermal system as it was not re-deposited in other rock-alteration types.

Potassium is highest in the central part of the ore system (K-silicate zone) where most samples contain excess of 2% wt. percent K_2O both titanium and phosphorus remain largely independent of alteration effects. The only significant reaction liberating Ti is a chloritization of biotite, when the element generally remains in situ as sphene and rutile. Maganese like Ca, is most markedly reduced in the innermost part of the biotite zone and increases in abundance outward. Unlike Ca, however, Mn mobilized during mineralization and K-silicate alteration processes was concentrated in the propylitic zone, where abundance are up to twice those of background levels in the volcanic.

Copper and sulfur are generally increased in all alteration assemblages and have clearly been added to the hydrothermal system as a whole. Copper exhibits the distribution already discussed with values in the potassic zone mostly in excess of 3000 ppm. Values in propylitic zone rocks show a wide range and are generally in excess of background abundances. Copper to sulphur ratios in the (chalcopyrite-rich) K-silicate alteration are much higher than in the propylitic (pyrite-rich) zone.

Trace elements: Rubidium shows an overall gradual increase toward the ore body to reach to maximum level in the biotite zone. Rubidium was clearly added along with K to the hydrothermal system during mineralization, alteration processes. Strontium shows the reverse effect and unlike Ca, mobilized Sr has apparently been accumulated in areas of propylitized granodiorite.

Rubidium to strontium ratio values show a more evident increase toward the ore body. Barium which exhibits varying dispersion pattern in the porphyry of the Darrehzar stock shows an apparent overall mobilization from altered intrusives into the surrounding intrusive and generally supports assertions. That Ba and Sr might represent geochemical tools in the search for ore bodies in volcanic rocks.

Both lead and Zinc show similar dispersion patterns respect to the ore zone. A distinct Zn (<50 ppm) and Pb (<3 ppm) low corresponds with the ore body with an apparent complementary halo in the fringing propylitic zone.

Zirconium and to a lesser extent Yttrium, show similar behavior to Pb and Zn. All three elements were apparently released by altering and mineralizing fluids in the central K-silicate zone and mobilized outward in to propylitic zone, where they were re-deposited.

DISCUSSION

Darrehzar has a complex intrusion, faulting, hydrothermal and alteration and mineralization indicated by field, petrographic, mineralogic and chemical studies. Sulfide mineralization in Darrehzar porphyry is ultimately linked to the process of hydrothermal alteration as shown by the spatial and genetic association and alteration occurred in two stages. The first stage is represented by the deposition of disseminated pyrite and minor amount of chalcopyrite and sphalerite in the pyrite-quartz-feldspar porphyry. This mode of mineralization is a result of the passage of an aqueous fluid through the rocks, leading to the exchange of components between the fluid and the rock. The second stage was mainly localized along fractures and is characterized by alteration assemblages and sulfide minerals. In the potassic alteration zone, the principal chemical changes were the enrichment of K and Ba and the depletion of Na, Ca, Mg, Mn and Fe. Mineralogically, these changes were accommodated by crystallization of K-feldspar and biotite at the expense of plagioclase and amphibole. The replacement of plagioclase and amphibole by K-feldspar and biotite, respectively, served to add K and remove Ca and Na. Depletion of Fe was due to the alteration of Fe-rich magmatic amphibole and biotite and phengitic muscovite with appreciably lower Fe/Fe+Mg ratios.

Phyllic alteration is superimposed on the potassic zone and is characterized by sericitization of feldspar. Compared to the potassic alteration zone, the phyllic alteration zone is depleted in Na, K, Fe and Ba and enriched of alkali feldspar and ferromagnesian minerals (e.g., hydrothermal biotite which had been formed during the potassic alteration), respectively. The addition of Si is consistent with the widespread silicification which is a major feature of phyllic alteration.

Barite was not found in the Darrehzar deposit and the only minerals that could accommodate Ba are K-feldspar and mica, which formed in potassically altered rocks. Copper added to potassically altered rock in significant amount, as might be expected from the dissemination of chalcopyrite and bornite in this zone.

CONCLUSIONS

- Immobile elements in water-rock interaction are useful in determining precursor to altered rocks and in calculating mass change during the alteration
- Change in major elements in potassic alteration zone, like enrichment in K and depletion in Na, Ca, Mn and Fe, are due to replacement of plagioclase and amphibole by K-feldspar and biotite, respectively

- Potassic alteration was associated with a large addition of Cu represented by disseminated chalcopyrite and bornite in this zone
- Propylitic alteration caused addition in Ca and reduction in SiO_2.
- Isocon plots illustrate that Al and TiO_2 were relatively immobile during alteration and that mass was essentially conserved
- Phyllic alteration was accompanied by depletion in Na, K, Fe and enrichment in Si and Cu
- The loss of Na, K and Fe reflects the sericitization of alkali feldspar and destruction of ferromagnesian minerals. The addition of Si is consistent with the widespread silicification which is major feature of phyllic alteration and the addition of Cu mobilized from the transition zone which is depleted in this element
- Hydrothermal alteration assemblages define concentric patterns centered on the inner part of the intrusion. These alteration zones vary from a potassic core through a well-developed phyllic shell a spot argillic zone and an outer propylitic fringe. The hypogene subeconomic copper mineralization (0.09%) occurs at the boundary between the potassic and the phyllic zones, in disseminations and in veins shallow supergene sulfide zone (0.04% Cu) in mainly located in the argillic alteration

ACKNOWLEDGMENTS

The researchers are grateful to Professor F. Moore and Dr. S. Liaghat for their constructive comments. This study benefited from discussions with Dr. A. Moradian, vice chancellor of college of sciences, Shahid Bahonar University. We appreciate the critical reading by the arbitration committee and we welcome any insightful comments and enlightening suggestions.

REFERENCES

Amidi, S.M., M.H. Emami and R. Michel, 1984. Alkaline character of Eocene volcanism in the middle part of Iran and its geodynamic situation. Geologischen Rundschau, 73: 917-932.

Atapour, H. and A. Aftabi, 2007. The geochemistry of gossans associated with sarcheshmeh porphyry copper deposit, Rafsanjan, Kerman, Iran: Implications for exploration and the environment. J. Geochemical Explor., 93: 47-65.

Berberian, M., 1995. Master blind thrust faults hidden under the Zagoros folds: Active basement tectonics and surface morphotectonics. Tectonophysics, 241: 193-224.

Derakhshani, R. and G. Farhoudi, 2005. Existence of the Oman line in the empty quarter of Saudi Arabia and its continuation in the Red Sea. J. Applied Sci., 5: 745-752.

Derakhshani, R. and M. Abdolzadeh, 2009. Mass change calculations during hydrothermal alteration/mineralization in the porphyry copper deposit of Darrehzar, Iran. Res. J. Environ. Sci., 3: 41-51.

Forster, H., 1978. Mesozoic-cenozoic metallogenesis in Iran. J. Geol. Soc. London, 135: 443-455.

Grant, J.A., 1986. The isocon diagram-a simple solution to gresens equation for metasomatic alteration. Econ. Geol., 81: 1967-1982.

Hezarkhani, A. and A. Jones, 1998. Control of alteration and mineralization in the Sungun porphyry copper deposit, Iran: Evidence from fluid inclusions and stable isotopes. Econ. Geol., 93: 651-670.

Hezarkhani, A., 2006a. Hydrothermal evolution of the Sar-Cheshmeh porphyry Cu-Mo deposit, Iran: Evidence from fluid inclusions. J. Asian Earth Sci., 28: 409-422.

Hezarkhani, A., 2006b. Mass changes during hydrothermal alteration/mineralization at the sar-cheshmeh porphyry copper deposit, Southeastern Iran. Int. Geol. Rev., 48: 841-860.

Honarmand, M., H. Ranjbar and Z. Moezifar, 2002. Integration and analysis of airborne geophysics and remote sensing data of sar cheshmeh area, using directed principal component analysis. Exploration Mining Geol., 11: 43-48.

Maclean, W.H., 1988. Rare earth elements mobility at constant inter REE ratios in the alteration zone at the phelps dodge massive sulfide deposit, Matagami, Quebec. Mineralium Deposita, 23: 231-238.

Rahnama, R.J., R. Derakhshani, G. Farhoudi and H. Ghorbani, 2008. Basement faults and their relationships to salt plugs in the Arabian platform in Southern Iran. J. Applied Sci., 8: 3235-3241.

Ranjbar, H., H. Hassanzadeh, M. Torbati and O. Ilaghi, 2001. Integration and analysis of airborne geophysical data of the Darrehzar area, Kerman Province, Iran, using principal component analysis. J. Applied Geophys., 48: 33-41.

Ranjbar, H., M. Honarmand and Z. Moezifar, 2004. Application of the crosta technique for porphyry copper alteration mapping, using ETM^+ data in the Southern part of the Iranian volcanic sedimentary belt. J. Asian Earth Sci., 24: 237-243.

Regard, V., O. Bellier, J.C. Thomas, M.R. Abbasi and J. Mercier *et al*., 2004. Accommodation of Arabia-Eurasia convergence in the Zagros-Makran transfer zone, SE Iran: A transition between collision and subduction through a young deforming system. Tectonics, 23: TC4007-TC4007.

Regard, V., O. Bellier, J.C. Thomas, D. Bourles and S. Bonnet, 2005. Copper mulative right-lateral fault slip rate across the zagros-makran transfer zone: Role of the minab-zendan fault system in accommodating Arabia-Eurasia convergence in Southeast Iran. Geophys. J. Int., 162: 177-203.

Shahabpour, J. and J.D. Kramers, 1987. Lead isotope data from the sarcheshmeh porphyry copper deposit, Iran. Mineralium Deposita, 22: 278-281.

Shahabpour, J. and M. Doorandish, 2008. Mine drainage water from the sar cheshmeh porphyry copper mine, Kerman, IR Iran. Environ. Monit. Assess., 141: 105-120.

Shahabpour, J., 1991. Some secondary ore formation features of the sar cheshmeh porphyry copper-molybdenum deposit, Kerman, Iran. Mineralium Deposita, 26: 275-280.

Talebian, M. and J. Jackson, 2002. Offset on Main recent fault of NW Iran and implication for the late Cenozoic tectonics of the Arabia-Eurasia collision zone. Geophys. J. Int., 150: 422-439.